Journal of Ovonic Research Vol. 11, No. 6, November - December 2015, p. 285 - 291

ELECTRICAL AND OPTICAL CHARACTERISTICS OF Sb-DOPED AND ANNEALED NANOCRYSTALLINE SnO_2 THIN FILMS DEPOSITED IN CBD TECHNIQUES

A. I. ONYIA[a,b], M. N. NNABUCHI[b]
[a]*Department of Industrial Physics, Enugu State University of Science and Technology, Enugu State, Nigeria*
[b]*Department of Industrial Physics, Ebonyi State University, Abakaliki, Nigeria*

Tin oxide (SnO_2) thin films doped with antimony were grown on plane glass substrates using chemical bath deposition (CBD) technique. Precursor chemicals of stannic chloride and sodium hydroxide were used to supply tin and oxygen ions respectively and triethanolamine (TEA) was added as a complexant. Sb doping was accomplished by adding little quantity antimony chloride that enabled orderly growth of ternary $Sn_{1-x}Sb_xO_2$ film where $0 < x < 0.1$. Synthesized films were annealed at temperatures of between 150℃ and 350℃ in steps of 50℃ for one hour at a time, and the effects on optical and electrical properties of film observed. Such high temperature treatment increased the energy band gap, E_g of films annealed at 150℃ but decreased such gap for films annealed at very high temperatures. Furthermore, the UV-VIS-NIR spectrophotometric analysis of films which provided E_g also showed high transmittance ($T > 80$ %) in visible region and also high absorbance ($A > 0.2$) in NIR. Annealing also increased electrical conductivity in all the temperatures considered.

(Received November 17, 2015; Accepted December 28, 2015)

Keywords: SnO_2, Complexant, Thin film, Band gap.

1. Introduction

In recent years, research in tin oxide (SnO_2) has regained prominence for its transparent conductive applications and its achievement of high conversion efficiencies in SnO_2/Si solar cells [1– 4]. But Stannic oxide thin film has low conductivity if undoped [5]. To improve its conductivity, indium has been the well established dopant which is used to produce the now popular indium tin oxide (ITO) thin film. But ITO is very expensive and scarce[6]. Different doping is therefore very pertinent to increase conductivity of SnO_2 at reasonable cost. Antimony doped tin oxide, i.e. Sb:SnO_2 or simply called Antimony Tin oxide (ATO) has gained prominence in this regards[7, 8] but using complicated techniques like DC Sputtering[9], Sol-gel process[10] and spray pyrolysis [11]. We have however found a way of using chemical bath deposition technique to fabricate ATO thin films of good optical and electrical characteristics by slowing down its precipitation rate with appropriate quantity of triethanolamine complexant.

2. Experimental Details

3.5ml of 1M $SnCl_4$ + 10.0ml of 0.5M NaOH and 2.0ml of triethanolamine (TEA) were added in 50ml beaker and distilled water was added to make up the solution up to 40ml that was stirred vigorously for few minutes. The chemical bath was raised to a temperature of 80℃ in an oven before dropping a plane glass substrate, preheated to 170℃, into the bath and supported by synthetic foam that rested on top of the beaker. The set up was left at this temperature(80 ℃) for

*Corresponding author : ikeaonyia@yahoo.com

32min after which the substrates, now covered with ATO, was removed, rinsed and drip dried in dust free environment. Sb doping was achieved by adding small quantity of $SbCl_3$ to the bath. Thin film formation was basically an oxidation process:

$$SnCl_4 + O_2 \longrightarrow SnO_2 + 2Cl_2$$

The TEA complexed the reaction to slowly precipitate SnO_2 as follows:

$$SnCl_4 + TEA \longrightarrow [Sn(TEA)]^{4+} + 4Cl^-$$
$$[Sn(TEA)]^{4+} \longrightarrow Sn^{4+} + TEA$$
$$2NaOH + 4OH^- \longrightarrow 2Na^+ + 3O^{2-} + 3H_2O$$
$$Sn^{4+} + 2O^{2-} \longrightarrow SnO_2$$

The ability to produce films of good crystal order depended critically on the temperatures of bath and initial temperatures of substrate as well as on the proper choice of variables that included concentrations and volumes of solutions used and time of deposition. Addition of dopant solution was done incrementally to achieve an optimally small percentage abundance of antimony that ensured highest film conductivity. Such percentage was deduced in Rutherford backscattering (RBS) analysis. The doped films were annealed for one hour at a time at varying temperatures of 150, 200, 250, 300 and 350 degree Centigrade and the effects on the electrical and optical properties were studied. Films were also passed through a UNICO-UV-2012PC spectrophotometric analysis to get the UV-VIS-NIR absorbance, A. From the data, transmittance, T, reflectance, R and absorption coefficient, α were generated using well known mathematical relation that connected them to film thickness, t[12]. Such thickness for each film was also deduced in RBS analysis. Electrical resistivity was measured using a Quadpro Model 301 auto calculating four point probe (FPP) and the level of crystallinity was confirmed in X-ray diffraction using a Philips X-Pert PRO Diffractometer that utilised Cu K_α radiator as choice X-ray of λ = 0.15406nm to scan films continuously from 2theta =10° - 99° in step size of 0.2° at room temperature of 288K.

3. Results and Discussion

3.1. Morphology

Morphology of as-grown film shows numerous voids and pinholes which however drastically reduced when film was annealed for an hour at 150℃. Development of small grains of the films into grid-like structure is easily noticeable in the annealed sample (Figure 2) suggesting the formation of nanostructured material [12]. This observed long network structural ordering made SnO_2 good light trappers for solar cells

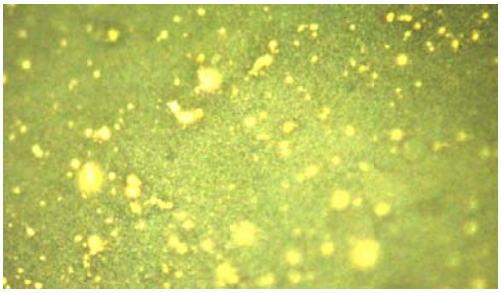

Fig. 1. Morphology of as-grown film (1000X)

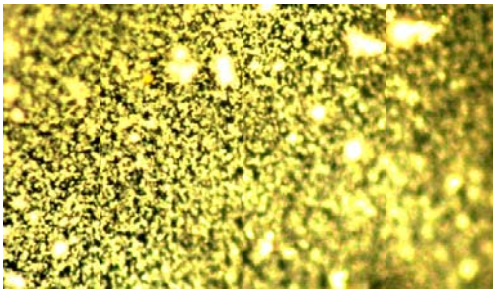

Fig. 2. Morphology of film annealed at 150℃ (1000X)

3.2. X-ray Diffraction Results

X-ray diffraction done on the films used a Philips X-Pert PRO Diffractometer that utilised Cu Kα radiator as choice X-ray of λ = 0.15406nm to scan films continuously from 2theta =10° - 99° in step size of 0.2° at room temperature of 288K. No discernible peaks were noticed for the as-grown film but clear peaks and pattern showed in the case of film annealed for an hour at 150 °C confirming that clear crystalline film was deposited. Diffraction lines were noticed at 2theta = 26.4˚, 29.7˚ and 51.2˚ and the patterns were matched to JCPDS data 05-0640 to make phase identification and decipher reflection planes, crystal angles and full width at half maximum (FWHM) from which Scherrer's rule[13] was applied to deduce the film grain size. Such planes were (110), (220) and (400) corresponding to the three lines respectively and the average grain size was 24.05nm. It appeared that a rapid pyrolysis growth of seed crystals initially took place on the pre-heated substrates and these seeds created growth patterns in the subsequent but more complexant-controlled precipitations at the chemical bath temperature.

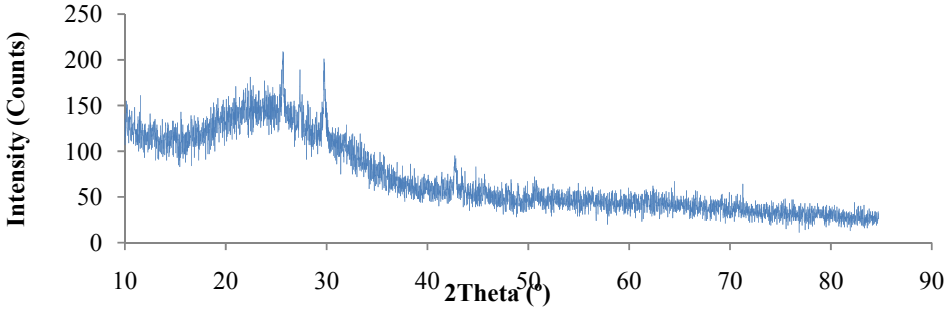

Fig. 4. XRD pattern for tin oxide thin film annealed at 150˚C

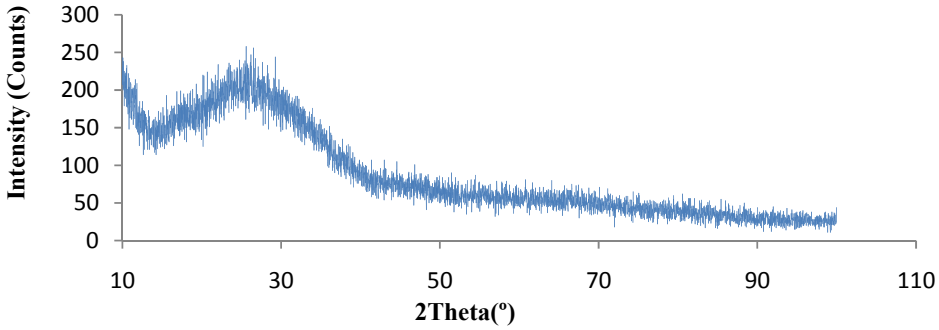

Fig. 3. XRD pattern for as-grown tin oxide thin film

3.3. Rutherford Backscattering Results

The result of Rutherford backscattering analysis for film annealed at 150 °C was as shown in figure 5 where a film of thickness 565nm lies over a substrate of 954740nm thick. The compositions of both the substrate and the deposit were also deciphered, and so also the elements percentage abundances.

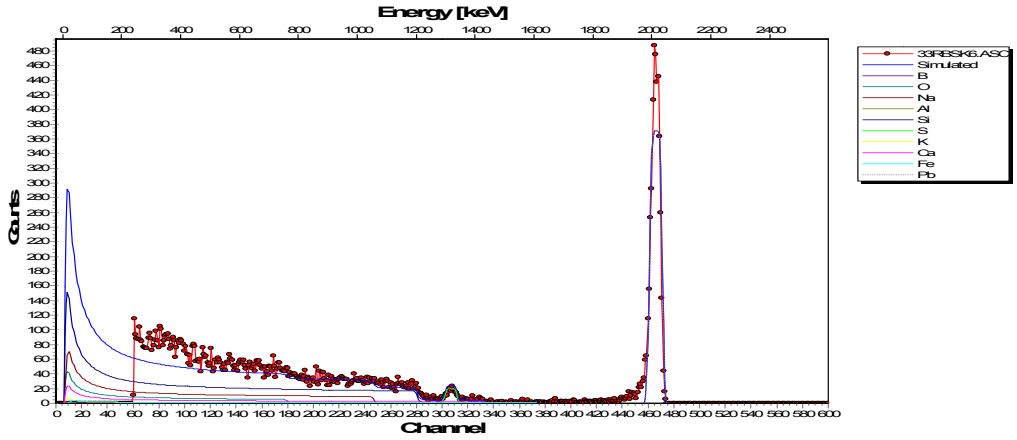

Fig. 5: RBS result of film. Layer 1:Thickness 565 nm. Compo: Sb 2.1%, Sn 40.3 %, O 58.0 %, Layer 2: Thickness 954740nm. Compo: Si 31.97%, O 32.89%, Na 25.85%, Ca 1.64%, Al 0.25%, K 1.05%, Fe 0.38%, B 5.89%.

3.4. Optical Results

Fig. 6 shows the result of spectroscopic absorption analysis where the legends in this and other graphs refer as follows:

1 As-grown thin film
2 Film annealed at 150 °C
3 Film annealed at 200 °C
4 Film annealed at 250 °C
5 Film annealed at 300 °C
6 Film annealed at 350 °C

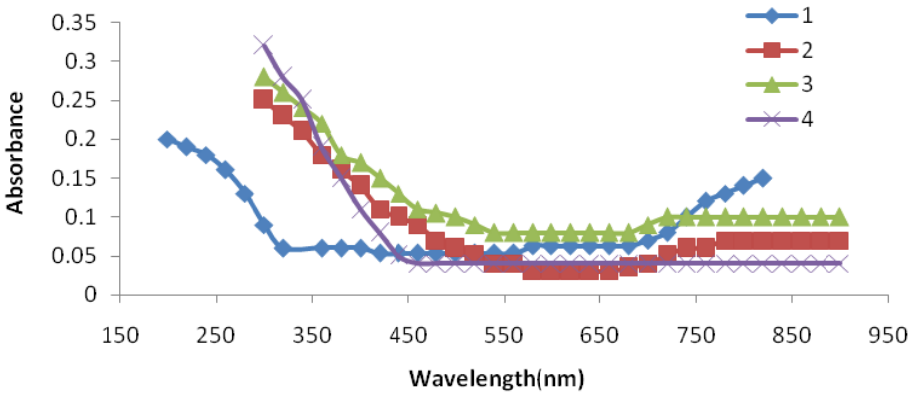

Fig. 6. Spectral absorbance ATO thin films

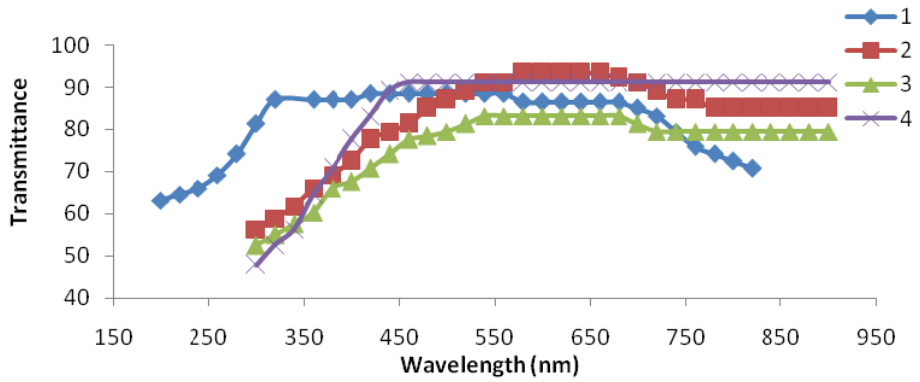

Fig. 7. Spectral transmittance of ATO thin films

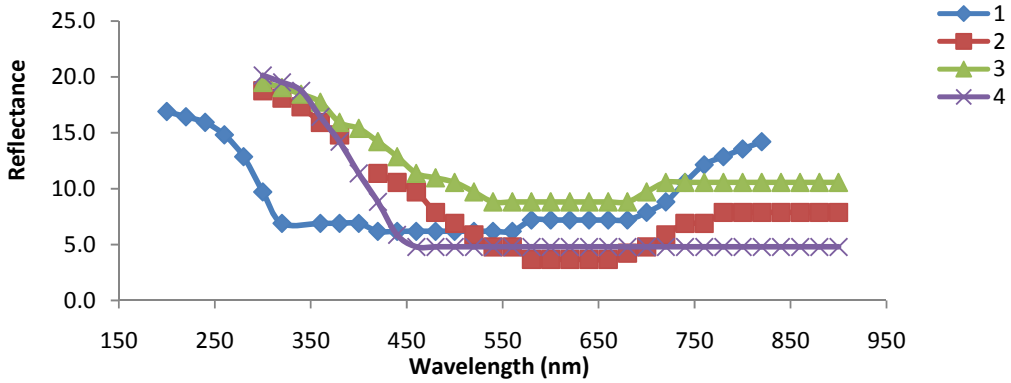

Fig. 8. Spectral reflectance of ATO thin films

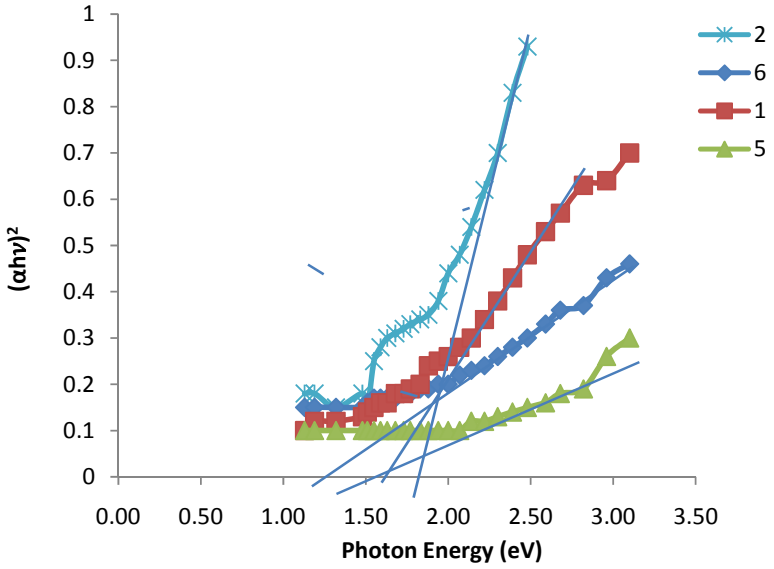

Fig. 9. Location of Energy gap of ATO

Table 1: Showing absorbance, A of ATO Films 1, 2, 3,and 4 at various broad frequencies of NIR(850nm), VIS(550nm) and near ultra violet[NUV](360nm).

	1	2	3	4
NIR	0.5	0.07	0.10	0.04
VIS	0.05	0.04	0.08	0.04
NUV	0.06	0.19	0.22	0.19

Table 2: showing R[T], ie Reflectance, R and Transmittance, T of ATO films 1, 2, 3 and 4.

	1	2	3	4
NIR	14.2[70.8]	7.9[85.1]	10.6[79.4]	4.8[64.6]
VIS	6.2[88.5]	4.8[91.2]	8.8[83.2]	4.8[91.2]
NUV	6.9[87.1]	16.4[66.1]	17.7[60.3]	16.4[64.6]

Figures 6, 7 and 8 show the absorbance, transmittance and reflectance spectra respectively of films 1 – 4. The summary of absorbance results for NIR(850nm), VIS(550nm) and NUV(360nm) is as shown in table 1 while that for reflectance and transmittance are shown in table 2. The relationship between the photon energy hν and film energy gap, E_g is given as:

$$\alpha h\nu = A(h\nu - E_g)^n \quad (1)$$

where A is a constant and n = ½ for direct allowed transition. This relation establishes that a plot of $(\alpha h\nu)^2$ versus hν produces a linear pattern the intercept on hν axis being the energy band gap, E_g of the thin film. The graph is however not linear at very low photon energies where, in general, lattice vibration absorption dominated this direct allowed transition. The extrapolations of the linear portions of graphs to the energy axis however deciphers such band gaps. Figure 9 shows the band gap of 1.60eV for as-grown film which increased to 1.80eV when film was annealed for an hour at 150 ^oC . Such increase continued for films annealed up till 250 ^oC before it decreased to 1.52eV for film annealed at 300 ^oC and still down to 1.34eV for film annealed at 350 ^oC . Using CBD techniques, other researchers have synthesized SnO2 thin films of comparable energy band gaps of 1.5eV – 2.2eV[1]. Our films were slightly but expectedly lower in resistivity as a result of Sb doping and annealing at high temperatures.

3.4. Electrical Characteristics

Four point probe (FPP) electrical resistivity results were as shown in figure 10 where resistivity of films decreased when film was initially annealed at higher temperatures. Such resistivity was 25 x 10-4Ωm for as-grown film and 15 x 10-4Ωm when film was annealed at 150 ^oC and 200 ^oC. Annealing at very high temperatures > 250 ^oC only increased film resistivity. It was thought that annealing at low temperatures oxidized some Sb3+ to Sb5+ and the excess electrons involved increased film conductivity by increasing the free carrier density. But further annealing at very high temperatures populated more Sb^{3+} ions thus decreasing film conductivity.

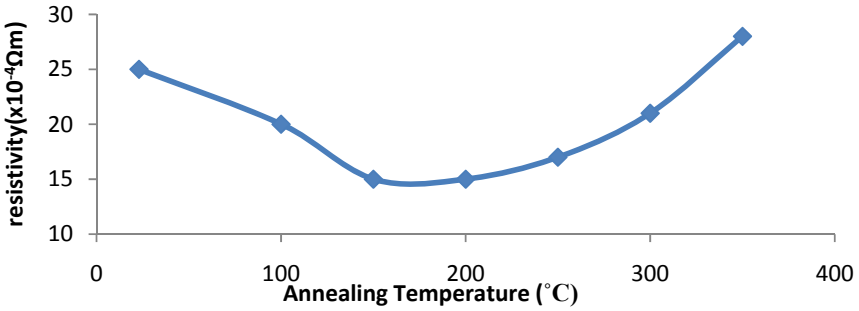

Fig. 10. Variation of film resistivity with annealing temperature

4. Conclusion

Sb-doped SnO_2 thin films were fabricated using chemical bath deposition technique. Such films showed good crystal order and low electrical resistivity when annealed between 100 ^oC and 250 ^oC. Such resistivity was dependent on annealing temperature with optimum value occurring at temperature of between 150 ^oC-200 ^oC. Energy band gaps of between 1.34 – 1.80eV were recorded for films that transmitted 63-91% the highest being in the VIS and the lowest being in the ultraviolet region. ATO thin films synthesized in this technique were comparable in qualities to reported ITO films and can be used as transparent conducting windows and as solar cell materials.

References

[1] M. Nwodo, S. C. Ezugwu, F. I. Ezema, P. U. Aogwa and R. U. Osuji, Journal of Optoelectronics and Biomedical Materials. **2(4)**, 267-272 (2010).
[2] G. Quin., D. Li, Z. Chan, Y. Von, Z. Feng and S. Liu, Computational Material Science **46**(2), 418- 424 (2009).
[3] A. R. Babar, S. S. Shinde, A.V. Moholkar, C. H. Bhosale, J. H. Kim, and K. Y. Rajpure, Journal of Semiconductors **32**(5), 1-8 (2011).
[4] P. U. Asogwa, S. C. Ezugwu, F. I. Ezema and R. U. Osuji, Chalcogenide Letters **6**(7), 287 (2009).
[5] D. Zhang, D. Deng, J. Zhang. and L. Chan, Material Chemistry and Physics **98**(2-3), 353-357 (2006).
[6] H. Liu, V. Aurutin, N. Izyumskaya, U. Ozgov and H. Morkoc, Superlattices and Micro-structures **48,** 458-484 (2010).
[7] M. Hemissi, H. Amardjia - Adnani, J. C. Plenet, B. Canut and J. M. Pelletier, Revue des Energies Renouvelables **10**(2), 273 – 279 (2007).
[8] L. U. Peng-Fei, Y. Shen, Y. U. Zhong-Yuan, L. Zhaq Long, L. I. Qiong-Yao, M. A. Shi-Jia, and L. I. U. Yu-Min, Commu. Theor. Phys. **57**(1), 145-150 (2012).
[9] S. Aydin, G. Turgut, M. Yilmaz, D. Tatar, B. Duzgun and M. Ertugrul**,** International Journal of the Physical Sciences **7**(34), 5327-5333 (2012).
[10] Y. B. Shen, T. Yamazaki, Z. F. Liu, C. J. Jin, T. Kikuta, and N. Nakatani, Thin Solid Films **516,** 5111 (2008).
[11] A. I. Onyia and C. E. Okeke, Journal of Physics D: Applied Physics, **22,** 1515 (1989).
[12] R. A. Chikwenze, Solution growth and characterization of binary selenide thin films for device applications (Unpublished doctoral thesis). University of Nigeria, Nsukka (2012).
[13] A. I. Onyia and M. N. Nnabuchi, Chalcogenide Letters **11**(9), 443-452 (2014).